Macromolecular Dynamics

An introductory lecture

Joachim Wuttke

Jülich Centre for Neutron Science at FRM II
Forschungszentrum Jülich GmbH

This text appeared in:
Macromolecular Systems in Soft and Living Matter, Lecture notes of the 42nd IFF Spring School 2011, edited by Jan K. G. Donth, Gerhard Gompper, Peter R. Lang, Dieter Richter, Marisol Ripoll, Dieter Willbold, Reiner Zorn.
Schriften des Forschungszentrums Jülich, ISBN 978-3-89336-688-0, Jülich 2011.

Contents

1 Systems and States

This lecture on polymer dynamics primarily addresses the molecular motion in melts and solutions. Other states like rubber or glass will be refered to briefly. Therefore, let us start by sorting out the following states of macromolecular matter:

A *polymer melt* is basically a liquid. However, in contrast to a *simple* liquid, its constituent molecules are flexible, and therefore their center-of-mass motion is usually accompanied by conformational changes. The dynamics is further complicated by the entanglement of neighbouring chain molecules. As a result, polymer melts are highly viscous and non-Newtonian liquids. The prime example for a naturally occuring polymer melt is latex, a milky fluid rich in cis-polyisoprene that is found in many plants, particularly abundant in the rubber tree.

A *rubber* (or *elastomer*) is obtained from a polymer melt by a chemical process called *vulcanization* that creates permanent inter-chain links. These cross-links prevent long-ranged diffusion and viscous flow. On short time and length scales, however, the polymer segments can move as freely as in a melt, which explains the characteristic elasticity of the rubber state. Everyday examples: erasers, car tyres. An unvulcanised polymer melt is said to be in a *rubber state* if the entanglement is so strong that the chains do not flow on the time scale of observation.

Plastic materials are either thermosetting or thermoplastic.

A *thermosetting plastic* is obtained by irreversibly creating strong chemical inter-chain links. Examples: bakelite, duroplast, epoxy resin.

Thermoplastic materials are obtained in a reversible manner by cooling a polymer melt. They can be either amorphous or semi-crystalline.

An *amorphous* solid is also called a *glass*, provided that it can be reversibly transformed into a liquid. This transformation is called the *glass transition*; it occurs at a loosely defined temperature T_g. Examples: poly(methyl methacrylate) (PMMA, plexiglas), polystyrene, polycarbonate.

In *semicrystalline* polymers, chains run through ordered and disordered domains. The ordered, crystalline domains exist up to a melting point T_m. They provide strong links between different chains. In the temperature range between T_g and T_m, the disordered domains provide flexibility. Example: polyethylene ($T_\mathrm{g} \simeq -100 \ldots -70°\mathrm{C}$, $T_\mathrm{m} \simeq 110 \ldots 140°\mathrm{C}$), used for foils and bags. Most other thermoplastics are typically employed below T_g. Example: polyethylene terephthalate (PET, $T_\mathrm{g} \simeq 75°\mathrm{C}$, $T_\mathrm{m} \simeq 260°\mathrm{C}$), used for bottles and textile fibers.

In a *polymer solution* the dilute macromolecules are always flexible. Therefore they behave as in a pure polymer melt, except that interactions between segments are modified by the presence of a solvent.

2 Brownian Motion

Almost all of polymer dynamics can be described by means of *classical mechanics*. Quantum mechanics seems relevant only for the explanation of certain low temperature anomalies that are beyond the scope of this lecture. Since we aim at understanding macroscopically relevant *average* properties of a large number of molecules, the appropriate methods are provided by *statistical mechanics*.

Some fundamental methods of classical statistical mechanics have been originally developped for the description of *Brownian motion* [1]. In this introductory section, we will review two of them: the *Langevin equation* for the evaluation of particle trajectories, and the *Smolu-*

chowski equation for a higher-level modelling in terms of probability densities. Both methods are ultimately equivalent, but depending on the application there can be a huge computational advantage in using the one or the other.[1]

2.1 The Langevin equation

We consider a colloidal (mesoscopic) particle P suspended in a liquid L. Molecules of L frequently collide with P, thereby exerting a random force $\boldsymbol{F}(t)$. On average the impacts from opposite directions cancel, so that

$$\langle \boldsymbol{F}(t) \rangle = 0. \tag{1}$$

For this reason it was long believed that $L - P$ collisions cannot be responsible for the random motion of P. By noting the analogy with the fluctuations of good or bad luck in gambling, Smoluchowski (1906) showed that this argument is fallacious: After n collisions, the expectation value of total momentum transfer is indeed 0, but for each single history of n collisions one can nevertheless expect with high probability that the momentum transfer has summed up to a value different from 0.

This *random walk* argument was put on a firm base by Langevin (1908).[2] Let us write down the Newtonian equation of motion for the center-of-mass coordinate $\boldsymbol{r}(t)$ of P:

$$m\partial_t^2 \boldsymbol{r} = -\zeta \partial_t \boldsymbol{r} + \boldsymbol{F}, \tag{2}$$

or for the velocity $\boldsymbol{v} = \partial_t \boldsymbol{r}$:

$$m\partial_t \boldsymbol{v} = -\zeta \boldsymbol{v} + \boldsymbol{F}. \tag{3}$$

If P is a spherical particle of radius a, and L has a shear viscosity η_s, then the *friction coefficient* is (Stokes 1851) [4, § 20]

$$\zeta = 6\pi\eta_\mathrm{s} a. \tag{4}$$

Eq. (3) can be easily integrated:

$$\boldsymbol{v}(t) = m^{-1} \int_{-\infty}^{t} \mathrm{d}t' \, \boldsymbol{F}(t') \mathrm{e}^{-(t-t')/\tau_m}. \tag{5}$$

P may be said to have a *memory* of past collisions that decays with a *relaxation time*

$$\tau_m := \frac{m}{\zeta}. \tag{6}$$

To compute averages like $\langle \boldsymbol{v}^2 \rangle$ we must now specify the expectation value of random force correlation. We assume that different Cartesian components of $\boldsymbol{F}$ are uncorrelated with each other, $\langle F_\alpha F_\beta \rangle = 0$ for $\alpha \neq \beta$, and that random forces acting at different times t, t' are uncorrelated. The second moment of $\boldsymbol{F}$ then takes the form

$$\langle F_\alpha(t) F_\beta(t') \rangle = A\delta_{\alpha\beta}\delta(t - t') \tag{7}$$

where the delta function is a convenient approximation for a memory function that extends over no more than the duration of one $L - P$ collision.

[1] The following is standard material, covered by many statistical mechanics textbooks and by a number of monographs. For Brownian motion, see e. g. [2], for the Langevin equation, [3].

[2] K. Razi Naqvi [arXiv:physics/052141v1] contests this received opinion, arguing that Langevin's "analysis is at best incomplete, and at worst a mere tautology."

By virtue of (1), the average velocity is $\langle \boldsymbol{v} \rangle = 0$. However, as argued above, for each single history of $\boldsymbol{F}$ one can expect that the integral in (5) results in a nonzero velocity. After a short calculation we find that the second moment has the time-independent value

$$\langle \boldsymbol{v}^2(t) \rangle = \frac{3A}{2m\zeta}. \tag{8}$$

On the other hand, this moment is well known from the equipartition theorem

$$\frac{m}{2} \langle \boldsymbol{v}^2 \rangle = \frac{3}{2} k_\mathrm{B} T, \tag{9}$$

so that we obtain the coefficient $A = 2k_\mathrm{B}T\zeta$ that was left unspecified in (7).

In the next step, we can compute the *mean squared displacement* of P within a time span t, which we will abbreviate as

$$\langle r^2(t) \rangle := \left\langle [\boldsymbol{r}(t) - \boldsymbol{r}(0)]^2 \right\rangle. \tag{10}$$

We determine $\boldsymbol{r}(t)$ by explicit integration of (5), and after *some* calculation [3] we find

$$\langle r^2(t) \rangle = 6Dt - 6D\tau_m \left(1 - \mathrm{e}^{-t/\tau_m}\right) \tag{11}$$

where we have introduced

$$D := \frac{k_\mathrm{B}T}{\zeta}. \tag{12}$$

From the long-time limit $\langle r^2(t) \rangle \simeq 6Dt$, we identify D as the *diffusion coefficient* (Sutherland 1905, Einstein 1905). In the opposite limit $t \ll \tau_m$, ballistic motion is found: $\langle r^2(t) \rangle \doteq \langle (\boldsymbol{v}(0)t)^2 \rangle$.

2.2 The Smoluchowski equation

Alternatively, Brownian motion can be analysed in terms of the space-time distribution $\rho(\boldsymbol{r}, t)$ of suspended particles. The continuity equation is

$$\partial_t \rho + \boldsymbol{\nabla} \boldsymbol{j} = 0. \tag{13}$$

As usual, the current $\boldsymbol{j}$ has a diffusive component (Fick 1855)

$$\boldsymbol{j}^\mathrm{diff} = -D\boldsymbol{\nabla}\rho. \tag{14}$$

We now assume that a potential $U(\boldsymbol{r})$ is acting upon the particles. In the stationary state, the force $-\boldsymbol{\nabla}U$ is just cancelled by the friction $-\zeta\vec{v}$. Accordingly, the drift component of $\boldsymbol{j}$ is

$$\boldsymbol{j}^\mathrm{drift} = \rho\boldsymbol{v} = -\zeta^{-1}\rho\boldsymbol{\nabla}U. \tag{15}$$

Collecting everything, we obtain the *Smoluchowski equation* (1915)

$$\partial_t \rho = D\boldsymbol{\nabla}^2\rho + \zeta^{-1}\boldsymbol{\nabla}(\rho\boldsymbol{\nabla}U). \tag{16}$$

For a velocity distribution or for the more general case of a phase-space distribution it is known as the *Fokker-Planck equation* (1914/1917).

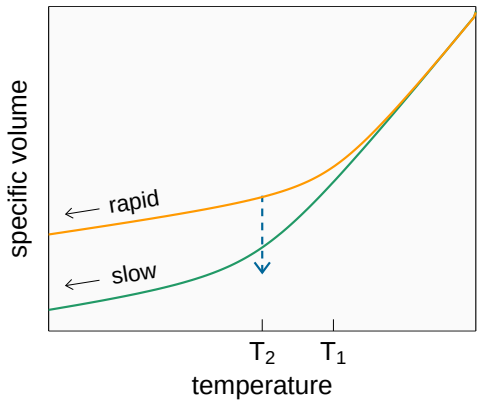

Fig. 1: *Temperature dependence of the specific volume of a glass forming system. Depending on the cooling rate, the cross-over from liquid-like to glass-like slopes is observed at different temperatures, and it results in different glass states. If the system is cooled rapidly to T_2 and then kept at that temperature, it relaxes towards states that are normally obtained by slow cooling. Similar behavior is found for the enthalpy.*

In the stationary state $\partial_t \rho = 0$, we expect to find a Boltzmann distribution $\rho \propto (-U/k_\mathrm{B}T)$. It is easily verified that this holds provided D and ζ are related by the *Sutherland-Einstein relation* (12). Combined with (4), the *Stokes-Einstein relation*

$$D = \frac{k_\mathrm{B}T}{6\pi\eta_\mathrm{s}a} \tag{17}$$

is obtained. Surprisingly, this relation holds not only for mesoscopic suspended particles, but even for the motion of one liquid molecule among others (the *hydrodynamic radius* a is then treated as an adjustable parameter). Only in the highly viscous supercooled state, the proportionality $D \propto T/\eta_\mathrm{s}$ is found to break down.

3 Segmental Relaxation and the Glass Transition

3.1 The glass transition

It is generally believed that the ground state of condensed matter is always an ordered one. However, in many supercooled liquids this ordered state is kinetically inaccessible. Crystallization through homogeneous nucleation requires the spontaneous formation of nuclei of a certain critical size. If the crystalline unit cell is complicated and the energy gain small, then this critical size is rather larger. If at the same time a high viscosity entails a low molecular mobility, then the formation of a stable nucleus may be so improbable that crystallization is practically excluded. On further supercooling the liquid becomes an amorphous solid, a *glass*.

Glass formation is observed in quite different classes of materials: in covalent networks like quartz glass (SiO_2) or industrial glass (SiO_2 with additives), in molecular liquids, in ionic mixtures, in aqueous solutions, and others. In polymers, glass formation is the rule, not the exception. As said in Sect. 1, some plastic materials are completely amorphous; in others crystalline domains are intercalated between amorphous regions.

The *glass transition* is *not* a usual thermodynamic phase transition of first or second order, as can be seen from the temperature dependence of enthalpy or density (Fig. 1): the cross-over

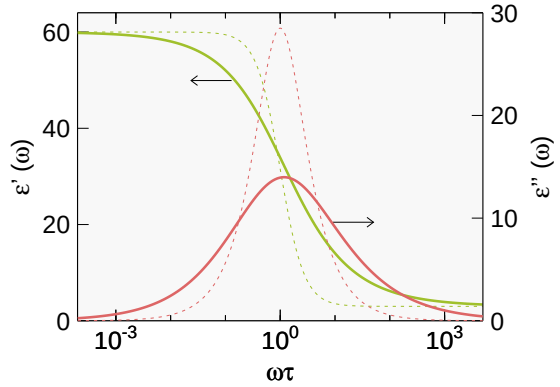

Fig. 2: *Dielectric spectrum in the viscous liquid or rubber state. As long as molecular dipoles are able to follow an external electric field modulation, the permittivity* $\epsilon(\omega) = \epsilon'(\omega) + i\epsilon''(\omega)$ *has the elevated low-frequency value of a polar liquid, here* $\epsilon_0 = 60$*. On the other hand, when probed with a high-frequency field modulation, dipoles appear frozen, resulting in the low permittivity of a solid, here* $\epsilon_\infty = 3$*. As required by the Kramers-Kronig relation, the dispersion of* $\epsilon'(\omega)$ *is accompanied by a dissipation peak in* $\epsilon''(\omega)$*. The dispersion step and the loss peak are* stretched *when compared to Debye's Eq. (82) (dashed).*

from liquid-like to solid-like slopes is smooth, and it depends on the cooling rate. When the cooling is interrupted within the transition range, *structural relaxation* towards a denser state is observed. This shows that glass is not an equilibrium state: on the contrary, it can be described as a liquid that has fallen out of equilibrium.[3]

3.2 Structural relaxation

Relaxation can also be probed by applying a periodic perturbation. This is done for instance in dielectric spectroscopy (Fig. 2). For reference, the most elementary theory of dielectric relaxation (Debye 1913) is derived in Appendix B. It leads to a complex permittivity

$$\epsilon(\omega) = \epsilon_\infty + \frac{(\epsilon_0 - \epsilon_\infty)}{(1 - (i\omega\tau)^\alpha)^\gamma} \tag{18}$$

with $\alpha = \gamma = 1$. Empirically the cross-over from liquid-like to solid-like behavior extends over a much wider frequency range than this formula predicts: it is *stretched*. Often, this stretching is well described if the exponents anticipated in Eq. (18) are allowed to take values below 1 (Cole, Cole 1941, Cole, Davidson 1951, Havriliak, Negami 1967). Alternatively (Williams, Watts 1970), $\epsilon(\omega)$ can be fitted by the Fourier transform of the *stretched exponential* function

$$\Phi_{\mathrm{K}}(t) = \exp(-(t/\tau)^\beta) \tag{19}$$

originally introduced to describe relaxation in the time domain (R. Kohlrausch 1854, F. Kohlrausch 1863).

[3] You may object that the supercooled liquid is already out of equilibrium — with respect to crystallization. However, the crystalline ground state is a null set in phase space: beyond nucleation it has no impact upon the dynamics of the liquid. The glass transition, in contrast, can be described as an ergodicity breaking in phase space.

The thermodynamics of the glass transition is subject of ongoing debate. A recent attempt to clarify confused concepts is [5].

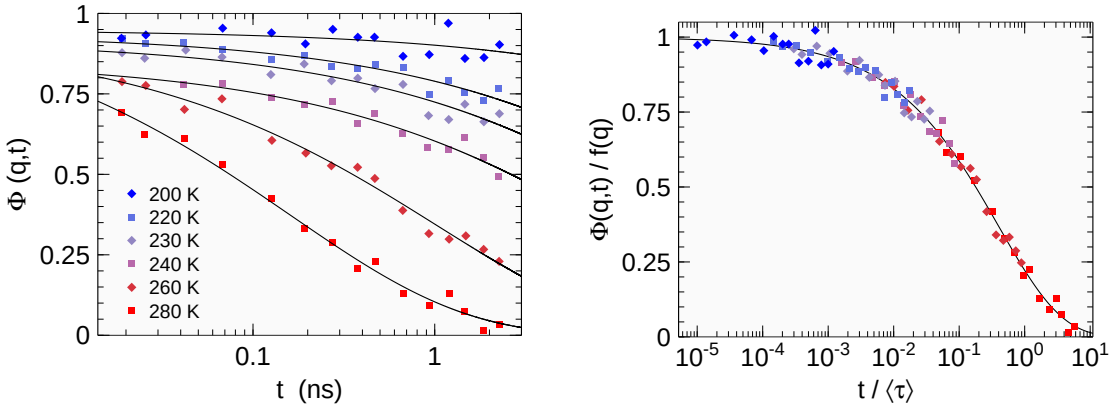

Fig. 3: *(a) Correlation function $\Phi(q,t)$ of deuterated polybutadiene, measured by neutron spin-echo at $q = 1.5\,\text{Å}^{-1}$ (close to the maximum of $S(q)$). Solid lines: fits with $f_q \exp(-(t/\tau)^\beta)$ with fixed $\beta = 0.45$. (b) Master curve. Data from [6].*

Generally, the relaxation time τ depends much stronger on temperature than the stretching exponents α, γ or β. This can be expressed as a *scaling law*, often called *time-temperature superposition principle*: Permittivities $\epsilon(\omega; T)$ measured at different temperatures T can be rescaled with times $\tau(T)$ to fall onto a common *master curve* $\hat{\epsilon}(\tau(T)\omega)$.

Quite similar results are obtained for other response functions. For instance, the longitudinal mechanic modulus, a linear combination of the more fundamental shear and bulk moduli, can be probed by ultrasonic propagation and attenuation in a kHz... MHz range, or by light scattering in a "hypersonic" GHz range (Brillouin 1922, Mandelstam 1926).

Particularly interesting is the pure shear modulus $G(\omega)$, which can be probed by torsional spectroscopy. Since a liquid cannot sustain static shear, there is no constant term in the low-frequency expansion

$$G(\omega) = i\eta\omega + \mathcal{O}(\omega^2). \tag{20}$$

The coefficient η is the macroscopic *shear viscosity*. If $G(\omega)$ obeys time-temperature superposition, then $\eta(T)$ is proportional to a shear relaxation time $\tau_\eta(T)$.

By virtue of the fluctuation-dissipation theorem (Appendix A), relaxations can also be studied *in* equilibrium, via correlation functions that can be measured in inelastic scattering experiments. Fig. 3 shows the normalized correlation function

$$\Phi(q,t) := S(q,t)/S(q,0) \tag{21}$$

of a glass-forming polymer, measured in the time domain by neutron spin echo. Scaling is demonstrated by construction of a master curve, stretching by fits with a Kohlrausch function.

3.3 Relaxation map and secondary relaxation

At this point it is interesting to compare the outcome of different experimental methods. It is found that the susceptibility master curve is not universal; different spectroscopies generally yield different stretching exponents. Relaxation times may vary by factors 2 or more. However, with good accuracy all relaxation times have the same *temperature dependence*. This is demonstrated in Fig. 4 for a particularly well studied molecular liquid. Upon cooling from 290 to 190 K, the relaxation times increase in parallel by almost 12 decades. When a viscosity of

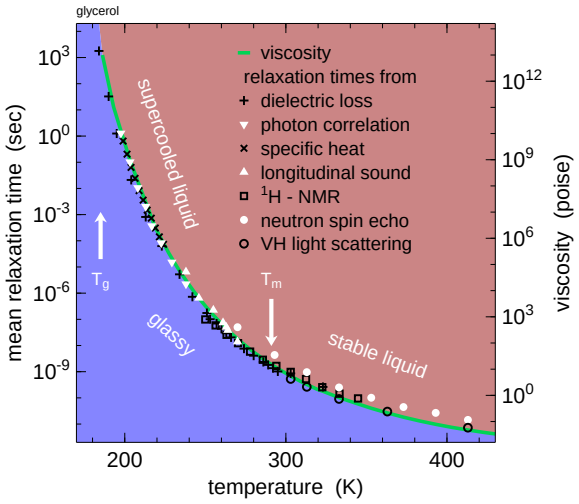

Fig. 4: *Relaxation times in glycerol, determined by various spectroscopies. This plot can be read as a* dynamic phase diagram: *whether the material reacts like a liquid or a solid depends not only on temperature, but also on the time scale of observation. Adapted from [7].*

10^{13} Poise (10^{12} Pa s) or a relaxation time of about 10^3 s is reached, relaxation falls out of equilibrium on the time scale of a human observer. As anticipated above, this is the glass transition. All relaxation modes that follow the temperature dependence of viscosity are conventionally called α relaxation.

The temperature dependence of relaxation times is often discussed with reference to the simplest physical model that comes to mind: thermally activated jumps over an energy barrier E_A,

$$\tau = \tau_0 \exp \frac{E_\mathrm{A}}{k_\mathrm{B} T} \tag{22}$$

(van t'Hoff 1884, Arrhenius 1889). Therefore, data are often plotted as $\log \tau$ versus $1/T$ or T_g/T so that a straight line is obtained if (22) holds. The α relaxation in glass forming liquids, however, almost never follows (22); its trace in the Arrhenius plot is more or less concave. Many fitting formulæ have been proposed; for most applications it is sufficient to extend (22) by just one more parameter, as in the Vogel-Fulcher-Tammann equation (for polymers also named after Williams, Landel, Ferry)

$$\tau = \tau_0 \exp \frac{A}{T - T_0}. \tag{23}$$

The singularity T_0 lies below T_g, and it is unclear whether it has any physical meaning.

In many materials, there is more than just one relaxation process. If the additional, *secondary* processes are faster than α relaxation, they are conventionally labelled $\beta, \gamma, \ldots$. In rarer cases, a slower process is found, designated as α' and tentatively explained by weak intermolecular associations. While γ and higher order relaxations are always attributed to innermolecular or side-chain motion, the situation is less clear for β relaxation. There are theoretical arguments (Goldstein 1969) and experimental findings (Johari 1970) to support the belief that β relaxation is a universal property of glass-forming systems. In any case, all secondary relaxations are well described by the Arrhenius law (22). This implies that at some temperature they merge with the α relaxation. This is well confirmed, principally by dielectric spectroscopy, which has the advantage of a particularly broad bandwidth. Fig. 5 shows an example for this merger or decoupling of α and β relaxation; such an Arrhenius plot is also called *relaxation map*.

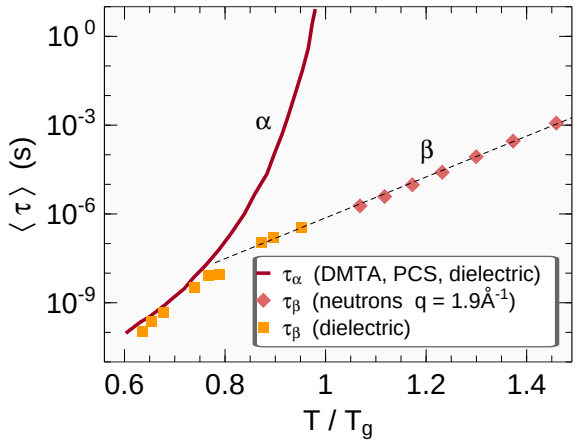

Fig. 5: *α and β relaxation times of cross-linked polyurethane, obtained by differential mechanical-thermal analysis (DMTA), photon correlation spectroscopy (PCS), dielectric spectroscopy and neutron scattering. Data from [8].*

3.4 The mode-coupling crossover

At present, there exists no satisfactory microscopic theory of relaxation near the glass transition. At moderate to low viscosities the situation is slightly better, since basic phenomena can be explained to some extent by a *mode-coupling theory* (Götze *et al.* 1984–).[4] This theory attacks the microscopic dynamics at the level of the normalized density pair correlation function (21). An equation of motion is written in the form

$$0 = \ddot{\Phi}_q(t) + \nu_q \dot{\Phi}_q(t) + \Omega_q^2 \Phi_q(t) + \Omega_q^2 \int_0^t \mathrm{d}\tau\, \dot{\Phi}_q(t-\tau) m_q\{\Phi(\tau)\}, \tag{24}$$

which guarantees that subsequent approximations do not violate conservation laws. In a systematic, though uncontrolled expansion the *memory kernel* m_q is then projected back onto products of pair correlations,

$$m_q\{\Phi(t)\} \simeq \sum_{k+p=q} V_{kpq}(T) \Phi_k(t) \Phi_p(t). \tag{25}$$

The coupling coeffients V_{kpq} depend only on the static structure factor $S(q)$, which in turn depends weakly on the temperature. This temperature dependence, however, is sufficient to trigger a transition from ergodic, liquid-like solutions to non-ergodic, glassy ones:

$$\begin{aligned} &\Phi_q(t \to \infty) \to 0 && \text{for } T > T_\mathrm{c}, \\ &\Phi_q(t \to \infty) \to f_q > 0 && \text{for } T < T_\mathrm{c}. \end{aligned} \tag{26}$$

On cooling towards T_c, a *critical slowing down* is predicted that is characterized by *two* diverging timescales,

$$\begin{aligned} t_\sigma &= t_0\, \sigma^{-1/(2a)}, \\ \tau_\sigma &= t_0\, \sigma^{-1/(2a)-1/(2b)}, \end{aligned} \tag{27}$$

with the reduced temperature $\sigma := T/T_\mathrm{c} - 1$. The microscopic timescale t_0 is of the order Ω_q^{-1}. The exponents fulfill $0 < a < b < 1$; they depend on just one lineshape parameter called λ.

[4] The standard reference for mode-coupling theory is the comprehensive book [9]. More accessible introductions are provided by [10, 11].

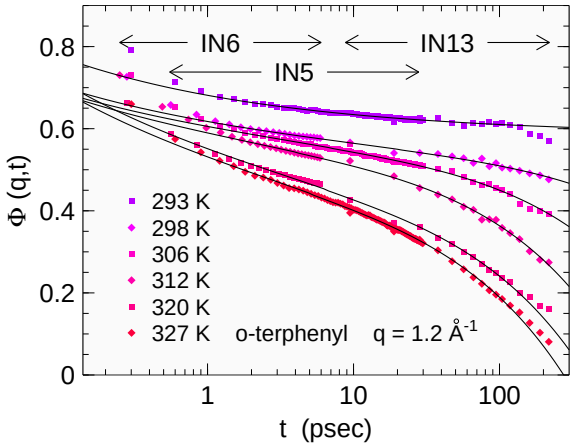

Fig. 6: *Incoherent intermediate scattering function $S_{\rm self}(q,t)$ of the molecular glass former ortho-terphenyl, obtained by combining Fourier transformed and resolution corrected neutron scattering spectra from three different spectrometers. Fits with the mode-coupling scaling law of fast β relaxation. Adapted from from [12].*

The pair correlation function passes through the following scaling regimes:

$$\begin{aligned} \Phi_q(t) &\simeq f_q + h_q\sigma^{1/2}(t/t_\sigma)^{-a} && \text{for } t_0 \ll t \ll t_\sigma, \\ \Phi_q(t) &\simeq f_q - h_q\sigma^{1/2}B(t/t_\sigma)^{b} && \text{for } t_\sigma \ll t \lesssim \tau_\sigma, \\ \Phi_q(t) &\simeq \hat{\Phi}_q(t/\tau_\sigma) && \text{for } \tau_\sigma \lesssim t. \end{aligned} \tag{28}$$

The regime delimited by the first two equations has been been given the unfortunate name "fast β relaxation" (the Johari-Goldstein process is then called "slow β relaxation" though it is faster than α relaxation).

The t^{-a} power law is a genuine theoretical prediction; it has been searched for in many scattering experiments, and it has actually shown up in a number of liquids. With the t^b power law, the theory explains experimental facts known since long (v. Schweidler 1907). This power law is also compatible with the short-time limit of Kohlrausch's stretched exponential; it leads over to the α relaxation master curve implied by the third equation of (28).

Mode-coupling predictions have been confirmed with impressive accuracy by light scattering studies of the density driven glass transition in colloidal suspensions (van Megen *et al.* 1991–). On the other hand, in conventional glass formers mode coupling is not the full story. By numerically solving simplified versions of (24), it is possible to fit relaxational spectra of normal or slightly supercooled liquids. On further supercooling, in favorable cases (such as shown in Fig. 6) the power law asymptotes of slow β relaxation appear, and extrapolations yield a consistent estimate of $T_{\rm c}$. Typically, this $T_{\rm c}$ is located 15% to 20% *above* $T_{\rm g}$. This implies that the ergodicity breaking of Eq. (26) does not explain the glass transition; nor does the power law (27) fit the divergence of viscosities or relaxation times near $T_{\rm g}$.

This leads to the view that $T_{\rm c}$ marks a *crossover* between two dynamic regimes: a mode-coupling regime at elevated temperature and low viscosity, and a "hopping" regime in highly viscous, deeply supercooled liquids. Experimental support for the significance of this crossover comes from a possible change in the functional form of $\eta(T)$ or $\tau(T)$, from the aforementioned breakdown of the Stokes-Einstein relation (17), and from the merger of α and slow β relaxation.

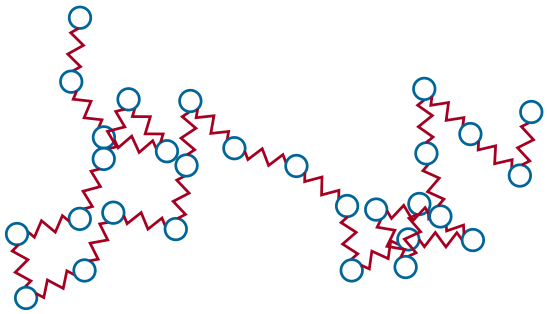

Fig. 7: *Spring-bead model of a flexible polymer. Since one bead represents several monomeric units, there is no preferential bond angle at the level of this model. Note also that the forces represented by the springs are entropic.*

4 Dynamics of a Free Chain

4.1 The spring-bead model

While the short-time dynamics of a polymer melt is quite similar to that of any other viscous liquid, on longer time scales the chain structure of the polymer makes a decisive difference, imposing strong constraints on the segmental motion. To study the motion of an entire chain, we neglect all details of chemical structure. We approximate the polymer as a sequence of N *beads* at positions $\boldsymbol{r}_n$ ($n = 1, \ldots, N$), connected by $N-1$ *springs*. Each bead represents several monomeric units so that there is no preferred bond angle (Kuhn 1934[?], Fig. 7).

The time-averaged equilibrium configuration of the polymer is assumed to be given by a Gaussian distribution of bead-to-bead vectors $\boldsymbol{r}_n - \boldsymbol{r}_{n-1}$,

$$P\{\boldsymbol{r}\} \propto \exp\left(-\kappa \sum_{n=2}^{N} (\boldsymbol{r}_n - \boldsymbol{r}_{n-1})^2\right), \tag{29}$$

where the force constant

$$\kappa := \frac{3k_\mathrm{B}T}{b^2} \tag{30}$$

ensures an average squared spring length of b^2.

The size of a polymer coil can be characterized by a mean squared radius. The most common measures are the *end-to-end distance* R_e,

$$R_\mathrm{e}^2 := \langle (\boldsymbol{r}_N - \boldsymbol{r}_1)^2 \rangle = Nb^2 \tag{31}$$

and the *gyration radius*

$$R_\mathrm{g}^2 := N^{-1} \sum_n \langle (\boldsymbol{r}_n - \boldsymbol{r}_\mathrm{G})^2 \rangle \simeq Nb^2/6, \tag{32}$$

with the center of mass

$$\boldsymbol{r}_\mathrm{G} := N^{-1} \sum \boldsymbol{r}_n \tag{33}$$

The expressions (31), (32) hold in polymer melts and in Θ solutions. In other cases, both expressions are still valid approximations if the factor N is replaced by $N^{2\nu}$. In good solvents, the exponent is $\nu = 3/5$.

4.2 The Rouse model

The Gaussian distribution (29) is based on the assumption that the free energy $A = U - TS$ is dominated by the entropy $S = k_\mathrm{B} \ln P$ so that the internal energy U can be neglected. Hence each bead experiences an entropic force

$$\boldsymbol{F}_n^\mathrm{coil} = -\frac{\partial}{\partial \boldsymbol{r}_n} A = -\kappa \left(-\boldsymbol{r}_{n-1} + 2\boldsymbol{r}_n - \boldsymbol{r}_{n+1}\right), \tag{34}$$

with obvious modifications for $n = 1, N$. This force strives to minimize the distances between beads, thereby maximizing the coiling of the polymer.

The coupling to the heat bath shall be modelled by a random force $\boldsymbol{F}_n^\mathrm{heat}$. Its second moment is given by an obvious extension of (7),

$$\langle F_{n\alpha}^\mathrm{heat}(t) F_{m\beta}^\mathrm{heat}(t')\rangle = 2\zeta k_\mathrm{B} T \delta_{nm}\delta_{\alpha\beta}\delta(t-t'). \tag{35}$$

Finally, moving beads experience a friction $-\zeta \partial_t \boldsymbol{r}_n$. These three forces make up the *Rouse model*, which is a key reference in polymer physics (Rouse 1953).[5] Accordingly, the Langevin equation is

$$m\partial_t^2 \boldsymbol{r}_n = -\zeta \partial_t \boldsymbol{r}_n + \boldsymbol{F}_n^\mathrm{coil} + \boldsymbol{F}_n^\mathrm{heat}. \tag{36}$$

In polymer solutions, the simple linear friction term is no longer adequate; it must be replaced by a *hydrodynamic interaction*. This interaction is handled reasonably well by a theory (Zimm 1956) outlined in Appendix C.

At this point, let us indicate some orders of magnitude. Assuming a spring length $b = 1$ nm and equating it with the hydrodynamic radius in (4), and assuming further a microscopic viscosity $\eta_\mathrm{s} \simeq 10$ Pa·s, we find a friction coefficient ζ of the order of 10^{-7} to 10^{-6} Ns/m, in agreement with empirical data for polyisobutylene, polymethyl acrylate and natural rubber [16]. Assuming a bead mass of 100 Da, the single-bead collision relaxation time (6) is $\tau_m = m/\zeta \simeq 10^{-18}$ s, which means that inertia is completely negligible on all relevant time scales. At $T = 300$ K, thermal motion is of the order $\langle v^2\rangle^{1/2} \simeq 300$ m/s, and the force constant is about $\kappa \simeq 10^{-2}$ N/m.

4.3 Rouse modes

We will solve (36) by transforming to normal coordinates. To begin, we note that there is no coupling whatsoever between the three Cartesian components. Therefore, we need to consider just one of them. Let us write x and f for an arbitrary component of $\boldsymbol{r}$ and $\boldsymbol{F}^\mathrm{heat}$. Then the Langevin equation reads

$$m\partial_t^2 x_n = -\zeta \partial_t x_n - \kappa \left(-x_{n-1} + 2x_n - x_{n+1}\right) + f_n. \tag{37}$$

Introducing the vector notation $\underline{x} := (x_1, \ldots, x_N)^\mathrm{T}$, Eq. (37) takes the form

$$m\partial_t^2 \underline{x} = -\zeta \partial_t \underline{x} - \kappa\, \underline{\underline{K}}\, \underline{x} + \underline{f} \tag{38}$$

[5] Rouse theory is covered in many text books, most often using a continuum approximation probably due to de Gennes [13]. The short but well written chapter in [10] comes with a nice selection of experimental results. Among dedicated polymer physics textbooks, I found [14] indispensable though largely indigestible for its coverage of computational details, and [15] inspiring though sometimes suspicious for its cursory outline of theory.

with the force matrix

$$\underline{\underline{K}} = \begin{pmatrix} +1 & -1 & 0 & \cdots & 0 & 0 \\ -1 & +2 & -1 & \ddots & 0 & 0 \\ 0 & -1 & +2 & \ddots & 0 & 0 \\ \vdots & \ddots & \ddots & \ddots & -1 & 0 \\ 0 & 0 & 0 & -1 & +2 & -1 \\ 0 & 0 & 0 & 0 & -1 & +1 \end{pmatrix}_{N\times N} . \tag{39}$$

The entries $+1$ at both extremities of the diagonal reflect the necessary modification of Eq. (37) for $n = 1, N$. In the well known derivation of phonon dispersion, this complication at the boundary is usually ignored or superseded by an unphysical periodicity. It is largely unknown that the correct $\underline{\underline{K}}$ can be diagonalized quite easily without any approximation. The eigenvalues are

$$\lambda_p = 2 - 2\cos\frac{p\pi}{N} = 4\sin^2\frac{p\pi}{2N}, \quad p = 0, \ldots, N-1, \tag{40}$$

and the normalized eigenvectors $\underline{\hat{v}}_p$ have components

$$\hat{v}_{pn} = \begin{cases} N^{-1/2} & \text{for } p = 0, \\ (N/2)^{-1/2}\cos\dfrac{p(n-\frac{1}{2})\pi}{N} & \text{for all other } p, \end{cases} \tag{41}$$

where $n = 1, \ldots, N$. The proof requires no more than a straightforward verification of $\underline{\underline{K}}\,\underline{\hat{v}}_p = \lambda_p \underline{\hat{v}}$. Collecting the normalized eigenvectors into an orthogonal matrix $\underline{\underline{A}} := (\underline{\hat{v}}_0, \ldots, \underline{\hat{v}}_{N-1})$, we introduce normal coordinates

$$\underline{\tilde{x}} := \underline{\underline{A}}^{\mathrm{T}}\underline{x}, \quad \underline{x} = \underline{\underline{A}}\,\underline{\tilde{x}}, \tag{42}$$

and similar for $\underline{f}$. It is easily seen that the average random force correlation (35) is still diagonal,

$$\langle \tilde{f}_p(t)\tilde{f}_q(t')\rangle = 2\zeta k_{\mathrm{B}}T\delta_{pq}\delta(t-t'). \tag{43}$$

In consequence, for each normal mode one obtains a decoupled Langevin equation

$$m\partial_t^2\tilde{x}_p = -\zeta\partial_t\tilde{x}_p - \kappa\lambda_p\tilde{x}_p + \tilde{f}_p. \tag{44}$$

At this point we must distinguish the eigenmode with the special eigenvalue $\lambda_0 = 0$ from all the others.

The eigenmode $p = 0$ describes the motion of the center of mass $\boldsymbol{r}_{\mathrm{G}} = N^{-1/2}\tilde{\boldsymbol{r}}_0$. Since $\lambda_0 = 0$, (44) is identical with the Langevin equation for Brownian motion (2). Accordingly, the long-time evolution of the mean squared displacement is $\langle r_{\mathrm{G}}^2(t)\rangle \simeq 6D_{\mathrm{R}}t$, where the macromolecular *Rouse diffusion coefficient* is given by a rescaled version of the Sutherland-Einstein relation (12):

$$D_{\mathrm{R}} = \frac{k_{\mathrm{B}}T}{\zeta N}. \tag{45}$$

Turning to the *Rouse modes* with $p > 0$, we neglect the inertial term in the Langevin equation (44). Integration is then straightforward:

$$\tilde{x}_p(t) = \zeta^{-1}\int_{-\infty}^{t} \mathrm{d}t'\, \mathrm{e}^{-(t-t')/\tau_p}\tilde{f}_p(t'), \tag{46}$$

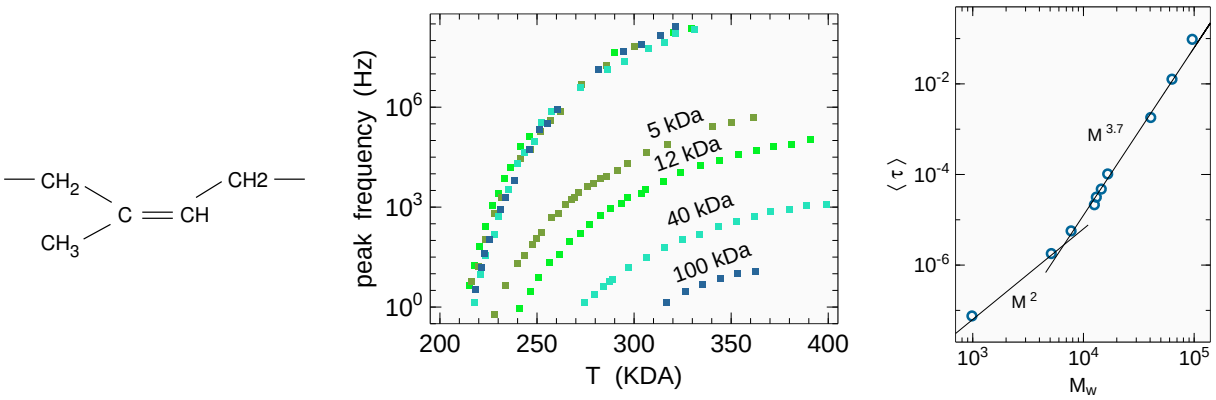

Fig. 8: *(a) Cis-polyisoprene consists of monomers that possess a dipole moment in direction of the polymeric bonds. (b) Peak frequencies ω of dielectric loss spectra in cis-polyisoprene samples of different molecular weight M. The normal mode resonance depends strongly on M, whereas the α relaxation does not. (c) Normal mode relaxation times $\tau = \omega^{-1}$ versus M, showing a crossover from the Rouse regime $\tau_\mathrm{R} \sim M^2$ to a stronger M dependence above the entanglement onset M_c. Data from [17].*

introducing the *mode relaxation time* $\tau_p := \zeta/(\kappa\lambda_p)$. It can be approximated for $p \ll N$ as

$$\tau_p \simeq \frac{\tau_\mathrm{R}}{p^2}. \tag{47}$$

The relaxation time of the fundamental mode $p = 1$ is known as the *Rouse time*:

$$\tau_\mathrm{R} := \frac{L^2\zeta}{3\pi^2 k_\mathrm{B}T}. \tag{48}$$

In this expression, N and b enter only via the *extended chain length* $L = Nb$, which does not change if we change our spring-bead model to consist of N/x segments of length bx. This justifies *ex post* that we have ignored all details of microscopic structure. A simple alternative expression for τ_R is

$$\tau_\mathrm{R} := \frac{2R_\mathrm{g}^2}{\pi^2 D_\mathrm{R}} \tag{49}$$

with the gyration radius (32).

4.4 Macroscopic consequences: dielectric and shear response

In favorable cases, Rouse relaxation can be observed by dielectric spectroscopy. In the simplest case, the monomeric possess a dielectric moment μ in direction of the polymeric bond. This requires the absence of a perpendicular mirror plane, which is the case e. g. for cis-polyisoprene (Fig. 8a). Then the overall dipole moment of the macromolecule is

$$\boldsymbol{\mu} = \sum_{n=2}^{N} (\boldsymbol{r}_n - \boldsymbol{r}_{n-1})\mu = (\boldsymbol{r}_N - \boldsymbol{r}_1)\mu \tag{50}$$

From (41) we infer that only eigenmodes with odd p contribute to (50). For $t \gtrsim \tau_\mathrm{R}$ pair correlations are dominated by the $p = 1$ mode:

$$\langle \boldsymbol{\mu}(0)\boldsymbol{\mu}(t)\rangle \propto \langle \tilde{\boldsymbol{r}}_1(0)\tilde{\boldsymbol{r}}_1(t)\rangle \propto \mathrm{e}^{-t/\tau_\mathrm{R}}. \tag{51}$$

According to the fluctuation-dissipation theorem (73), this correlation is proportional to a linear response function. After Fourier transform, one finds that the dielectric permittivity $\epsilon(\omega)$ has a Debye resonance around $\omega \sim \tau_{\mathrm{R}}^{-1}$.

Fig. 8b,c shows results of dielectric spectroscopy in cis-polyisoprene melts with different extended chain lengths $L = Nb$. In experimental reports the chain length is of course expressed as molecular weight M. The α relaxation peak, discussed above in Sect. 3.2, is perfectly independent of M, which confirms that it is due to innersegmental motion, In contrast, the normal mode relaxation time depends strongly on M. For low M, the Rouse prediction $\tau_R \sim M^2$ is confirmed. However, at $M_c \simeq 10$ kDalton, there is a rather sharp crossover to a steeper power law $M^{3.7}$ that is ascribed to entanglement effects.

Mechanical spectroscopy has the advantage that it works also if monomers are too symmetric for dielectric measurements. As already mentioned in Sect. 3.2 *torsional spectroscopy* probes a system's response to *shear*. Not seldom this response is nonlinear, due to non-Newtonian flow phenomena that are beyond the scope of the present lecture. As long as the response is linear, it can be described by the frequency dependent *shear modulus* $G(\omega)$. Its high frequency limit G_∞ quantifies the shear needed to cause a given *strain*. In a *liquid*, the low frequency limit G_0 is zero: stationary shear is not able to build up a lasting stress. Sometimes this is seen as the defining property of the liquid state. Instead of stationary shear, a flow gradient is needed to maintain strain. The proportionality coefficient is the *shear viscosity* η, which is the low frequency limit of $G(\omega)/(i\omega)$, as anticipated in (20).

To calculate $G(\omega)$ in the frame of Rouse theory, it is convenient to invoke a *Green-Kubo relation* (a variant of the fluctuation-dissipation theorem) according to which $G(\omega)$ is proportional to the Fourier transform of a stress autocorrelation function $\langle \sigma_{xz}(t)\sigma_{xz}(0)\rangle$.[6] The stress component σ_{xz} can be expressed through the displacements of individual beads. For weak elongations, the autocorrelation can be factorized so that $G(t)$ is proportional to the square of a normalized one-dimensional displacement autocorrelation function

$$\sum_n \frac{\langle \delta x_n(t)\delta x_n(0)\rangle}{\langle \delta x_n^2\rangle} = \sum_{p\geq 1} \frac{\langle \tilde{x}_p(t)\tilde{x}_p(0)\rangle}{\langle \tilde{x}_p^2\rangle}. \tag{52}$$

Using (46) to compute the normal mode autocorrelation we find

$$G(t) \sim \sum_p \mathrm{e}^{-2t/\tau_p}. \tag{53}$$

With $\tau_p \propto p^{-2}$ and replacing the sum by an integral we obtain the approximation

$$G(t) \sim \sum_{p\geq 1} \mathrm{e}^{-2p^2 t/\tau_{\mathrm{R}}} \sim \int_0^\infty \mathrm{d}p\, \mathrm{e}^{-2p^2 t/\tau_{\mathrm{R}}} \sim \left(\frac{\tau_{\mathrm{R}}}{t}\right)^{1/2}. \tag{54}$$

Fourier transform yields the power law

$$G(\omega) \sim \omega^{1/2}. \tag{55}$$

For small t, quite many eigenmodes contribute to (53) so that neither the low-p expansion (47) nor the extension of the summation to ∞ are justified. Therefore $G(\omega)$ must cross over from (55) to a constant high-frequency limit G_∞.

[6] The following is no more than a speculative summary of obscure calculations in [14] and [15].

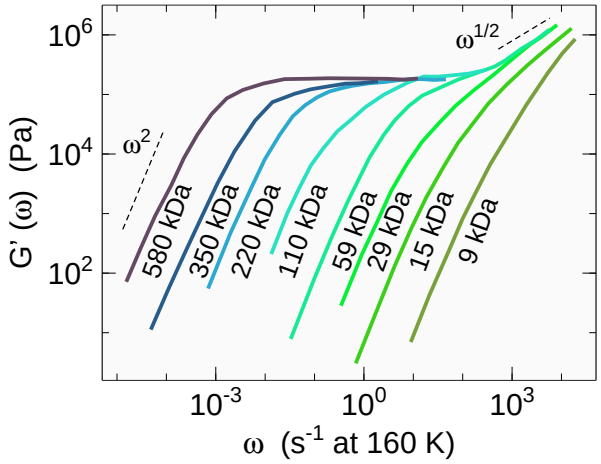

Fig. 9: *Real part $G'(\omega)$ of the shear modulus of polystyrene samples with different narrow molecular weight distributions. Experiments were done in a frequency range from $10^{-1.5}$ to $10^{0.5}$ s^{-1} and in a temperature range from 120 to 260 K. Then, time-temperature superposition was used to construct the master curves shown here. Data from [18].*

For large t, only few eigenmodes contribute to (53) so that the passage to a continuous p becomes invalid. In this case, it is more appropriate to compute the Fourier transform term by term, which yields a sum of Maxwell-Debye resonances

$$G(\omega) \sim \sum_p \frac{1}{1 - i\omega\tau_p}. \tag{56}$$

In the low-frequency limit we obtain a constant term of doubtful significance plus a linear term proportional to the viscosity

$$\eta \sim \sum \tau_p \sim \tau_{\mathrm{R}}. \tag{57}$$

From (48), we have $\tau_{\mathrm{R}} \sim N^2$, but there is a prefactor N^{-1} in $G(\omega)$ omitted in our sloppy derivation so that finally the Rouse model predicts $\eta \sim N$.

In Fig. 9 experimental data are shown. For moderate chain lengths, $G'(\omega)$ is indeed found to cross over from ω^2 (the lowest non-constant real term in the expansion of (56) to $\omega^{1/2}$. The ultimate limit G_∞ has not been reached in this experiment. For longer polymer chains, a flat plateau appears between the liquid-like ω^2 and the Rouse regime $\omega^{1/2}$. Such a constant value of $G(\omega)$ implies instantaneous, memory-free response, which is characteristic of rubber elasticity; it is caused by entanglement.

4.5 Microscopic verification: neutron spin echo

For direct, microscopic measurement of chain conformation fluctuations one must access length and time scales of the order of nm and ns. The most powerful instrument in this domain is the *neutron spin echo* spectrometer. The recent book [19] provides a comprehensive review of spin echo studies on polymer dynamics.

Usually, spin echo experiments require deuterated samples to avoid the otherwise dominant incoherent scattering from protons. The experiments then yield the *coherent dynamic structure factor* $S(q,t)$. However, for a simple, intuitive data analysis the *incoherent* scattering function $S_{\mathrm{i}}(q,t)$ is preferable. It is also denoted $S_{\mathrm{self}}(q,t)$ since it reveals the *self correlation* of a

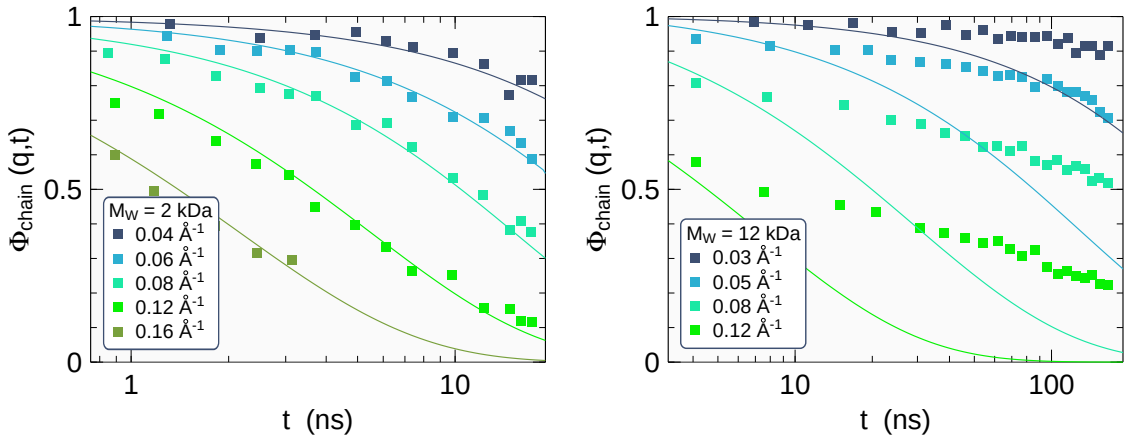

Fig. 10: *Single-chain coherent normalized dynamic structure factor of polyethylene melts at 509 K. Lines are predictions of the Rouse model. They fit for short chains (left), but not for long chains (right); note the different time scales. Data points and lines from [19].*

tagged particle. In *Gaussian approximation*

$$S_{\mathrm{i}}(q,t) = \langle \exp\left(iq(\boldsymbol{r}(t) - \boldsymbol{r}(0))\right)\rangle \simeq \exp\left(-q^2\langle r^2(t)\rangle/6\right), \tag{58}$$

it yields the mean squared displacement (10).

Measuring $S_{\mathrm{i}}(q,t)$ by neutron spin echo is difficult because the random spin flips associated with incoherent scattering destroy 2/3 of the incoming polarization. Nevertheless, thanks to progress in instrumentation, it is nowadays possible to obtain self correlation functions from undeuterated ("protonated") samples in decent quality. Alternatively, self correlations can be measured with the data quality of coherent scattering if short protonated sequences are intercalated at random in deuterated chains.

Within the Rouse model, and neglecting ballistic short-time terms, the mean squared displacement is given by

$$\langle r^2(t)\rangle = \frac{6}{N}\sum_{p=0}^{N-1}\left[\langle\tilde{\boldsymbol{x}}_p^2\rangle - \langle\tilde{\boldsymbol{x}}_p(t)\tilde{\boldsymbol{x}}_p(0)\rangle\right] = 6D_{\mathrm{R}}\left\{t + \sum_{p=1}^{N-1}\tau_p\left[1-\mathrm{e}^{-t/\tau_p}\right]\right\}. \tag{59}$$

With the same technique as in (54), one obtains the approximation

$$\langle r^2(t)\rangle \simeq 6D_{\mathrm{R}}\left\{t + (\pi\tau_{\mathrm{R}}t)^{1/2}\right\}. \tag{60}$$

At about $t \sim \tau_{\mathrm{R}}$, there is a cross-over from a $t^{1/2}$ regime dominated by conformational fluctuations to the t^1 diffusion limit. Inserting the asymptotic $\langle r^2(t)\rangle \sim t^{1/2}$ into (58) one obtains an expression that agrees with the Kohlrausch function (19) with a stretching exponent $\beta = 1/2$. This indicates that the high-p limit of the Rouse modes is more physical than might have been expected; it seems to capture even some aspects of segmental α relaxation. Be that as it may, the $t^{1/2}$ prediction has been impressively confirmed in neutron scattering experiments.

The *coherent* dynamic structure factor is more involved than (58). In general, it contains contributions from interchain as well as from intrachain correlations. Single-chain dynamics can be isolated by *contrast variation*, using a mixture of about 10% protonated and 90% deuterated polymer. Fig. 10 shows the single-chain dynamic structure factor of two polyethylene

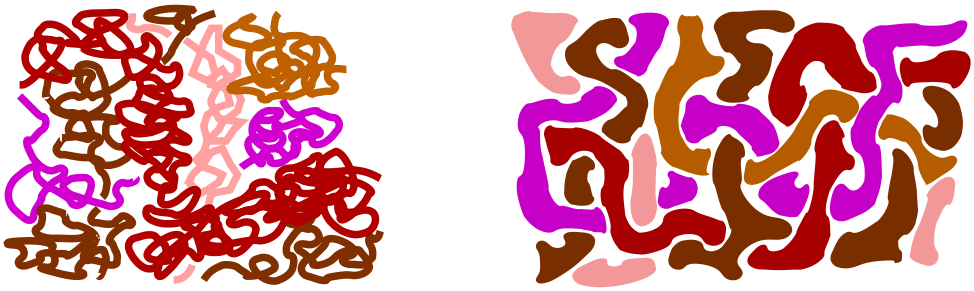

Fig. 11: *Entanglement. (a) Local detail, with relatively few chain crossings. (b) Coarse grained representation, showing heavy entanglement. Each monochrome, tube-like region is filled with coiled subunits of the polymer. For times between the entanglement time t_e and the disentanglement time t_d, polymer motion is confined to these tubes.*

melts with different chain lengths [19]. For short chains, the data are in perfect agreement with the Rouse model. For long chains, however, correlations decay much slower than predicted by the Rouse model. This is yet another indication of entanglement.

5 Entanglement and Reptation

Entanglement means that the conformational dynamics of a chain is hindered by presence of other chains. Entanglement is a topological constraint, due to the simple fact that chains cannot cross each other (Fig. 11). We have already encountered experimental results that provide clear evidence for the relevance of entanglement for polymer chains that exceed a certain size N_c:

- The dielectric relaxation time crosses over from the Rouse behavior $\tau \propto N^2$ (48) to a steeper slope $\tau \propto N^{3.7}$ (Fig. 8c).
- In the shear modulus $G(\omega)$, there appears a plateau $G(\omega) = \text{const}$ with rubber-like elasticity between the liquid limit $G(\omega) \simeq i\eta\omega$ and the Rouse regime $G(\omega) \sim \omega^{1/2}$ (Fig. 9).
- Neutron scattering shows that correlations within long chains decay much slower than predicted by the Rouse model (Fig. 10).

The rather sharp crossover at N_c implies that entanglement becomes relevant if the coil radius $N^{1/2}b$ (up to a constant factor, depending on definition) exceeds a certain value

$$a := N_\mathrm{c}^{1/2} b. \tag{61}$$

Up to this length scale, the chains are heavily coiled with little mutual penetration (Fig. 11a). On larger scales, the coarse-grained polymer chains have the character of heavily entangled *tubes* (Fig. 11b). Each tube can be modelled as an ideal random chain, consisting of beads of size a.

An *entanglement time* t_e can be defined by $\langle r^2(t_\mathrm{e})\rangle \simeq a^2$. Using (60) in the limit $t \ll \tau_\mathrm{R}$, we find up to numeric prefactors

$$t_\mathrm{e} \sim \frac{L_\mathrm{c}^2}{D} \tag{62}$$

with the critical extended chain length $L_\mathrm{c} = N_\mathrm{c} b$. For times beyond t_e, the dynamics is qualitatively different from the free chain Rouse regime. Since a chain is basically confined to a tube, it can only perform a one-dimensional, snake-like motion, called *reptation* (de Gennes 1971).

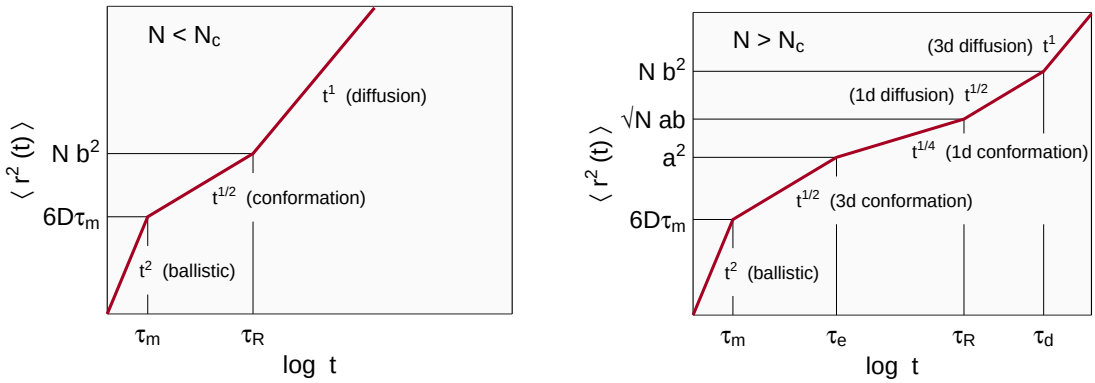

Fig. 12: *Time evolution of the mean squared displacement (10) on a double logarithmic scale. (a) For short chains, as predicted by Rouse theory. (b) For long chains, as predicted by de Gennes' reptation theory.*

For a short outline of some scaling results, we concentrate on the mean squared displacement. We will see that there are altogether no less than five different regimes. They are summarized in Fig. 12.

The one-dimensional dynamics within a tube shall be described by the Rouse model as before. Let s be a coordinate along the tube. The mean squared displacement in s is just one third of the Rouse result (60) in $\boldsymbol{r}$. Since the tubes are ideal Gaussian random coils, an extended tube length $s^2 = N_s^2 a^2$ corresponds to a squared real-space displacement of $r^2 = N_s a^2 = as$. In the *reptation* regime $t_\mathrm{e} \ll t \ll t_\mathrm{R}$ we obtain, omitting prefactors,

$$\langle r^2(t)\rangle \sim a D_\mathrm{R}^{1/2} (\tau_R t)^{1/4}. \tag{63}$$

This $t^{1/4}$ law is a key prediction of reptation theory; it has been confirmed by neutron spin echo measurements [19].

For times beyond t_R, the one-dimensional dynamics crosses over from innerchain Rouse fluctuations to center-of-mass diffusion. Accordingly, the real-space mean squared displacement takes the form

$$\langle r^2(t)\rangle \sim a D_\mathrm{R}^{1/2} t^{1/2}. \tag{64}$$

This holds until the chain escapes from its tube, which happens when $s^2 \sim N^2 b^2$ or $r^2 \sim aD_\mathrm{R} t_\mathrm{d}^{1/2}$. Using again $r^2 = as$, we obtain the *disentanglement time*

$$t_\mathrm{d} \sim \frac{N^3 b^2}{D}. \tag{65}$$

Finally, on time scales above t_d, the chain, having diffused out of its original tube, is free to try new conformations in three dimensions. This is a center-of-mass random walk, described by

$$\langle r^2(t)\rangle \simeq 6 D_\mathrm{d} t. \tag{66}$$

Matching (66) with (64) at t_d, we obtain the *disentangled diffusion coefficient*

$$D_\mathrm{d} \sim \frac{aD}{bN^2}. \tag{67}$$

The scaling laws $t_\mathrm{d} \sim N^3$ and $D_\mathrm{d} \sim N^{-2}$ are important predictions. The disentanglement time t_d determines the relaxation time τ observed in dielectric or mechanical spectroscopy. Empirically, the molecular mass dependence of τ is even stronger than N^3. Typical exponents are 3.2 to 3.6; in Fig. 8c we had even 3.7. This discrepancy shows that one-dimensional diffusion in fixed tubes is not the full story. It is necessary to take into account fluctuations of the neighbouring chains (*contour length fluctuations*). On the other hand, the prediction $D_\mathrm{d} \sim N^{-2}$ has been confirmed by quite direct, spatially resolved diffusion measurements [15].

Appendices

A Linear response theory: relaxation, dissipation, fluctuation

If a multi-particle system is exposed to a weak perturbation A, its response B is linear in A, as far as amplitudes are concerned. However, the response may be delayed in time, assuming the character of *relaxation*. Relaxation may be probed in time or in frequency, by spectroscopy (response to external perturbation) or by scattering methods (fluctuations in equilibrium). The relations between these probes are the subject of *linear response theory*, to be briefly summarized in this appendix.

The linear response $B(t)$ to a perturbation $A(t)$ can be written as

$$B(t) = \int_{-\infty}^{t} \mathrm{d}t'\, R(t-t')\, A(t'). \tag{68}$$

Consider first the momentary perturbation $A(t) = \delta(t)$. The response is $B(t) = R(t)$. Therefore, the memory kernel R is identified as the *response function*.

Consider next a perturbation $A(t) = \mathrm{e}^{\eta t}\Theta(-t)$ that is slowly switched on and suddenly switched off (Θ is the Heavyside step function, η is sent to 0^+ at the end of the calculation). For $t > 0$, one obtains $B(t) = \Phi(t)$ where Φ is the negative primitive of the response function,

$$R(t) = -\partial_t \Phi(t). \tag{69}$$

Since Φ describes the time evolution after an external perturbation has been switched off, it is called the *relaxation function*. In the special case of exponential (Lorentzian) relaxation, R and Φ are equal (up to a constant factor), which is a frequent source of confusion.

Consider finally a periodic perturbation that is switched on adiabatically, $A(t) = \exp(-i\omega t + \eta t)$, implying again the limit $\eta \to 0^+$. The response can be written $B(t) = \chi(\omega)A(t)$, introducing a *dynamic susceptibility*

$$\chi(\omega) := \int_0^\infty \mathrm{d}t\, \mathrm{e}^{i(\omega+i\eta)t}\, R(t). \tag{70}$$

This motivates the definition

$$F(\omega) := \int_0^\infty \mathrm{d}t\, \mathrm{e}^{i\omega t}\, \Phi(t). \tag{71}$$

of the one-sided Fourier transform $F(\omega)$ of the relaxation function $\Phi(t)$. Because of (69), there is a simple relation between χ and F:

$$\chi(\omega) = \Phi(0) + i\omega F(\omega). \tag{72}$$

In consequence, the *imaginary* part of the susceptibility, which typically describes the loss peak in a spectroscopic experiment, is given by the *real* part of the Fourier transform of the relaxation function, Im $\chi = \omega$Re $F(\omega)$. Conversely, *dispersion* is described by Re $\chi = \Phi(0) - \omega$Im $F(\omega)$.

Up to this point, the only physical input has been Eq. (68). To make a connection with *correlation functions*, more substantial input is needed. Using the full apparatus of statistical mechanics (Poisson brackets, Liouville equation, Boltzmann distribution, Yvon's theorem), it is found [20] that for classical systems

$$\langle A(t)B(0)\rangle = k_{\mathrm{B}}T\Phi(t). \tag{73}$$

This is an expression of the *fluctuation-dissipation theorem* (Nyquist 1928, Callen, Welton 1951): the left side describes fluctuations *in* equilibrium; the right side relaxation *towards* equilibrium, which is inevitably accompanied by *dissipation* (loss peak in Im χ).

Pair correlation functions are typically measured in *scattering* experiments. For instance, inelastic neutron scattering at wavenumber q measures the scattering law $S(q,\omega)$, which is the Fourier transform of the density correlation function,

$$S(q,\omega) = \frac{1}{2\pi}\int_{-\infty}^{\infty} \mathrm{d}t\, \mathrm{e}^{i\omega t}\langle \rho(q,t)^*\rho(q,0)\rangle. \tag{74}$$

In contrast to (71) and (70), this is a normal, two-sided Fourier transform. In consequence, if we let $\langle \rho(q,t)^*\rho(q,0)\rangle = \Phi(t)$, then the scattering law $S(q,\omega)$ is proportional to the real part Re $F(\omega)$ of the one-sided Fourier transform of $\Phi(t)$.

B Debye's theory of dielectric relaxation

In modern terms, Debye's theory of dipolar relaxation is based on a Smoluchowski equation that describes the time evolution of the probability distribution $f(\vartheta,\phi,t)$ of dipole orientations ϑ,ϕ ($0 \le \vartheta \le \pi$, $0 \le \phi < 2\pi$):

$$\zeta\partial_t f = \nabla(\beta^{-1}\nabla f + U\nabla f) \tag{75}$$

where ζ is a friction coefficient, U is an external potential, and $\beta \equiv 1/(k_{\mathrm{B}}T)$. Inserting spherical coordinates, ignoring ϕ, and keeping r constant, we obtain

$$\zeta'\partial_t f = (\sin\vartheta)^{-1}\partial_\vartheta \sin\vartheta(\beta^{-1}\partial_\vartheta f + f\partial_\vartheta U) \tag{76}$$

with $\zeta' = r^2\zeta$. An electric field in z direction causes a potential

$$U(t) = -\mu E(t)\cos\vartheta \tag{77}$$

that is proportional to the dipole moment μ.

With the ansatz

$$f(\vartheta,t) = 1 + \beta g(t)\cos\vartheta, \tag{78}$$

and introducing the *relaxation time* $\tau := \beta\zeta'/2$, Eq. (76) simplifies to

$$\tau\partial_t g(t) = -g(t) + \mu E(t) + \mathcal{O}(g\beta\mu E). \tag{79}$$

Under realistic experimental conditions, we always have $\mu E \ll \beta^{-1}$ so that the last term is negligible. The remaining linear differential equation shall be rewritten for a macroscopic observable, the polarization

$$P(t) = \int \frac{\mathrm{d}\Omega}{4\pi}\, \mu \cos\vartheta f(\vartheta, t) = \frac{\mu\beta g(t)}{3}. \tag{80}$$

We obtain

$$(1 + \tau\partial_t)P(t) = \frac{\mu^2\beta}{3}E(t). \tag{81}$$

In the simplest time-dependent experiment, the electric field is adiabatically switched on, then suddenly switched off at $t = 0$. The polarization then relaxes exponentially, $P(t) \propto \exp(-t/\tau)$. In a frequency-dependent experiment, a periodic perturbation $E(t) \propto \exp(i\omega t)$ is applied. This yields the *susceptibility*

$$\chi_{\mathrm{dipolar}}(\omega) = \frac{P(\omega)}{E(\omega)} = \frac{1}{1 - i\omega\tau}. \tag{82}$$

The relative electric permittivity is then

$$\epsilon(\omega) = 1 + \chi_{\mathrm{dipolar}}(\omega) + \chi_{\mathrm{other}}(\omega) \tag{83}$$

where the "other" contribution comes mainly from the electronic polarizability. The dashed lines in Fig. 2 show the *dispersion* step in the real part $\epsilon'(\omega)$ and the *dissipation* maximum in the imaginary part $\epsilon''(\omega)$.

C Zimm's theory of chain dynamics in solution

Starting with equation (34), the entire Rouse model is based on the assumption that the chain conformation is driven by entropy only. This a good approximation for melts, but generally not for solutions, except in the Θ condition. To account for the *swelling* of a polymer in solution, one needs at least to model the mutual sterical exclusion of different chain segments. The simplest approximation for this *excluded volume interaction* is the repulsive potential

$$U_{\mathrm{ex}}\{\boldsymbol{r}\} = k_{\mathrm{B}}T v_{\mathrm{ex}} \sum_{n\neq m} \delta(\boldsymbol{r}_n - \boldsymbol{r}_m). \tag{84}$$

As described in Sect. 4.1, its effect upon the equilibrium structure is limited to the modification of the exponent ν in the scaling laws (31), (32) for the coil radius.

For the *dynamics*, another modification of the Rouse model is even more important: one has to include the *hydrodynamic interaction* between the polymer and the solvent. The motion of a polymer bead drags the surrounding solvent with it, thereby creating a flow pattern, which in turn exerts a force upon other beads. If inertia is neglected, the friction term assumed in the Rouse model implies $\boldsymbol{v} = \zeta^{-1}\boldsymbol{F}$. To account for hydrodynamic interactions, this equation must be replaced by

$$\boldsymbol{v}_n = \sum_m \boldsymbol{H}_{nm}\boldsymbol{F}_m. \tag{85}$$

To estimate the coupling coefficients $\boldsymbol{H}_{nm}$, one usually refers to a simple case for which the hydrodynamic interaction can be obtained from first principles: for a point particle, located at

$\boldsymbol{r}_1(t)$ and dragged by a force $\boldsymbol{F}_1$, one can solve the Navier-Stokes equations to obtain the flow field $\boldsymbol{v}(r) = \boldsymbol{H}(\boldsymbol{r} - \boldsymbol{r}_1)\boldsymbol{F}_1$ with the *Oseen tensor*[7]

$$\boldsymbol{H}(\boldsymbol{r}) = \frac{1}{8\pi\eta r}\left(\mathbf{1} + \hat{\boldsymbol{r}} \otimes \hat{\boldsymbol{r}}\right), \tag{86}$$

which is then used to approximate

$$\boldsymbol{H}_{nm} \simeq \begin{cases} \zeta^{-1}\mathbf{1} & \text{for } n = m, \\ \boldsymbol{H}(\boldsymbol{r}_n - \boldsymbol{r}_m) & \text{else.} \end{cases} \tag{87}$$

Unfortunately, the $\boldsymbol{r}$ dependence of $\boldsymbol{H}$ makes the modified Langevin equation nonlinear. This obstacle is overcome in the *Zimm theory* (1956) by a *preaveraging* step that is basically a mean field approximation: $\boldsymbol{H}_{nm}$ is replaced by its average under the equilibrium distribution $P\{\boldsymbol{r}\}$. In the Θ condition, one obtains for $n \neq m$

$$\langle \boldsymbol{H}_{nm} \rangle \simeq \frac{\mathbf{1}}{(6\pi^3|n-m|)^{1/2}\eta b}, \tag{88}$$

which is a rather long-ranged interaction. In other conditions, a modified distribution $P\{\boldsymbol{r}\}$ might be used, leading to a modified power law $|n-m|^{-\nu}$.

The preaveraging linearization allows to rewrite the one-dimensional Rouse mode Langevin equation (44) with hydrodynamic interaction as

$$\partial_t \underline{\tilde{x}} = \underline{\underline{\tilde{H}}}\left(-m\partial_t^2 \underline{\tilde{x}} - \kappa\, \underline{\underline{\Lambda}}\, \underline{\tilde{x}} + \underline{\tilde{f}}\right) \tag{89}$$

with the diagonal matrix $\Lambda_{pq} = \delta_{pq}\lambda_p$ and with $\underline{\underline{\tilde{H}}} = \underline{\underline{A}}^{\mathrm{T}}\, \underline{\underline{H}}\, \underline{\underline{A}}$, which in the Θ condition is in good approximation

$$\tilde{H}_{pq} \simeq \begin{cases} 0 & \text{for } p \neq q, \\ \dfrac{8N^{1/2}}{3(6\pi^3)^{1/2}\eta b} & \text{for } p = q = 0, \\ \dfrac{N^{1/2}}{(3\pi^3 p)^{1/2}\eta b} & \text{else.} \end{cases} \tag{90}$$

For the $p = 0$ eigenmode, we find again Brownian motion, with the Zimm diffusion constant

$$D_{\mathrm{Z}} = \frac{k_{\mathrm{B}}T H_{00}}{N} \propto N^{-1/2}, \tag{91}$$

which differs from $D_{\mathrm{R}} \sim N^{-1}$ in the Rouse model. Allowing for excluded volume interaction in a good solvent, the aforementioned generalisation of (88) leads to $D_{\mathrm{Z}} \sim N^{-\nu}$. Comparing with (32), we find that the diffusion constant is in both cases determined by the coil radius: $D_{\mathrm{Z}} \sim R^{-1}$. This result is routinely used in *photon correlation spectroscopy* (somewhat misleadingly also called *dynamic light scattering*), where the diffusion coefficient of dilute macromolecules is measured in order to determine their gyration radius.

[7] I am unable to trace back this result to C. W. Oseen whose 1910 papers in Ark. Mat. Astr. Fys. are frankly unreadable. Zimm (1956) takes the tensor from Kirkwood and Riseman (1948) who cite a report by Burgers (1938) that is not easily available.

For nonzero eigenmodes, the Rouse time is replaced in the Θ condition by

$$\tau_{\mathrm{Z}} := \frac{\eta b^3 N^{3/2}}{(3\pi)^{1/2} k_{\mathrm{B}} T}, \tag{92}$$

and the mode relaxation times become

$$\tau_p \simeq \frac{\tau_{\mathrm{Z}}}{p^{3/2}}. \tag{93}$$

Again, the N dependence can be generalized towards a dependence on the coil radius, $\tau_{\mathrm{Z}} \sim R^3$.

References

[1] B. Duplantier, Séminaire Poincaré **1**, 155 (2005).

[2] R. M. Mazo, *Brownian Motion. Fluctuations, Dynamics, and Applications*, Oxford University Press: Oxford (2002).

[3] W. T. Coffey, Yu. P. Kalmykov, and J. T. Waldron, *The Langevin Equation*, World Scientific: Singapore (^{2}2004).

[4] L. D. Landau and E. M. Lifshitz, *Course of Theoretical Physics. Vol 6. Fluid Mechanics*. Translated from Russian, also available in other languages.

[5] L. Leuzzi and T. M. Nieuwenhuizen, *Thermodynamics of the Glassy State*, Taylor & Francis: New York (2008).

[6] D. Richter, B. Frick and B. Farago, Phys. Rev. Lett. **61**, 2465 (1988).

[7] J. Wuttke, Adv. Solid State Phys. (Festkörperprobleme) **40**, 481 (2000).

[8] C. Levelut, A. Faivre, J. Pelous, B. Johnson and D. Durand, **276–278**, 431 (2000).

[9] W. Götze, *Complex Dynamics of Glass-Forming Liquids. A Mode-Coupling Theory*, Oxford University Press: Oxford (2009).

[10] K. Binder and W. Kob, *Glassy Materials and Disordered Solids: An Introduction to their Statistical Mechanics*, World Scientific: Singapore (2005).

[11] T. Voigtmann, in *Soft Matter. From Synthetic to Biological Materials*, edited by J. K. G. Dhont *et al.* (Lecture Notes of the 39th Spring School), Forschungszentrum Jülich: Jülich (2008).

[12] J. Wuttke, M. Kiebel, E. Bartsch, F. Fujara, W. Petry and H. Sillescu, Z. Phys. B **91**, 357 (1993).

[13] P.-G. de Gennes, *Scaling Concepts in Polymer Physics*, Cornell University Press: Ithaca (1979).

[14] M. Doi and S. F. Edwards, *The Theory of Polymer Dynamics*, Clarendon: Oxford (1986).

[15] G. Strobl, *The Physics of Polymers*, Springer: Berlin (1996).

[16] J. D. Ferry, *Viscoelastic Properties of Polymers*, J. Wiley: New York (1961, ^{3}1980).

[17] D. Boese and F. Kremer, Macromolecules **23**, 829 (1990).

[18] S. Onogi, T. Masuda and K. Kitagawa, Macromolecules **3**, 109 (1970).

[19] D. Richter, M. Monkenbusch, A. Arbe and J. Colmenero, *Neutron Spin Echo in Polymer Systems* (Adv. Polym. Sci., Vol. 174), Springer: Berlin (2005).

[20] R. Kubo, Rep. Progr. Phys. **29**, 255 (1966).